

Wildfire potential evaluation during a drought event with a regional climate model and NDVI

Yongqiang Liu*, John Stanturf, Scott Goodrick

Center for Forest Disturbance Science, USDA Forest Service, Athens, Georgia, USA

ARTICLE INFO

Article history:

Received 1 February 2010

Received in revised form 29 March 2010

Accepted 3 April 2010

Keywords:

Regional climate modeling

Wildfire potential

Drought

KBDI

Soil moisture

NDVI

ABSTRACT

Regional climate modeling is a technique for simulating high-resolution physical processes in the atmosphere, soil and vegetation. It can be used to evaluate wildfire potential by either providing meteorological conditions for computation of fire indices or predicting soil moisture as a direct measure of fire potential. This study examines these roles using a regional climate model (RCM) for the drought and wildfire events in 1988 in the northern United States. The National Center for Atmospheric Research regional climate model (RegCM) was used to conduct simulations of a summer month in each year from 1988 to 1995. The simulated precipitation and maximum surface air temperature were used to calculate the Keetch–Byram Drought Index (KBDI), which is a popular fire potential index. We found that the KBDI increased significantly under the simulated drought condition. The corresponding fire potential was upgraded from moderate for a normal year to high level for the drought year. High fire potential is often an indicator for occurrence of intense and extensive wildfires. Fire potential changed in the opposite direction for the 1993 flood event, indicating little possibility of severe wildfires. The soil moisture and KBDI evaluations under the drought and flood conditions are in agreement with satellite remotely sensed vegetation conditions and the actual wildfire activity. The precipitation anomaly was a more important contributor to the KBDI changes than temperature anomaly. The small magnitude of the simulated soil moisture anomalies during the drought event did not provide sufficient evidence for the role of simulated soil moisture as a direct measure of wildfire potential.

Published by Elsevier B.V.

1. Introduction

Tens of thousands of wildfires occur annually in the United States. On average during the period from 1960 to 2008, more than 4 million acres (1.6 million ha) of forest and other ecosystems burned annually (NIFC, 2010). Severe wildfires are a natural disaster that threatens human life and property. In 2000, for example, wildfires consumed 8.4 millions of acres (3.4 million ha). Nearly 30 thousand people were involved in wildland firefighting efforts, with suppression costs to the federal government \$1.4 billion in one year alone. Wildfires also have environmental consequences including effects on atmospheric processes. Emissions from wildfires are an important source for atmospheric carbon (Dixon and Krankina, 1993; Amiro et al., 2001). For example, the carbon emissions from the 1997–98 Indonesian wildfires were the equivalent of the total global carbon uptake by the terrestrial biosphere in a typical year (Page et al., 2002; Tacconi et al., 2007). Furthermore, smoke particles are a source of atmospheric aerosols, which affect atmospheric radiative transfer through scattering and absorbing solar radiation and modifying cloud microphysics

(Charlson et al., 1992). These processes can further modify clouds and precipitation and atmospheric circulation (Ackerman et al., 2000; Liu, 2005a, 2005b). In addition, wildfires release large amounts of particulate matter and other air pollutants, which can degrade air quality and impact human health (Riebau and Fox, 2001).

Wildfires have significant inter-annual variability. For example, the burned area in the U.S. increased from 1.3 millions of acres (0.5 million ha) in 1998 to 5.6 millions of acres (2.3 million ha) the next year (NIFC, 2010). This mainly resulted from the inter-annual variability of atmospheric condition, which is a determinant for wildfires along with fuel properties and topography (Pyne et al., 1996). Severe wildfires usually occur under extreme weather conditions such as drought. Dry, hot, and windy weather combined with sufficient dry vegetation provides favorable conditions for fires to ignite and spread. Several researchers have successfully correlated long-term atmospheric anomalies and wildfire activity. For example, an analysis of reconstructed long-term fire and drought indices indicated that annual areas burned for the southwestern U.S. were associated with similar large-scale patterns in anomalously dry conditions (Westerling and Swetnam, 2003). The close relationship between droughts and wildfires provides a basis for evaluating and predicting wildfire potential. This is critical for fire planning, suppression implementation, and mitigating negative environmental effects.

* Corresponding author. Center for Forest Disturbance Science, US Forest Service, 320 Green St., Athens, Georgia 30602, USA. Tel.: +1 706 559 4240; fax: +1 706 559 4317.
E-mail address: yliu@fs.fed.us (Y. Liu).

Several techniques have been developed to evaluate wildfire potential including drought indices such as the Palmer Drought Severity Index (PDSI) (Palmer, 1965), the Keetch–Byram Drought Index (KBDI) (Keetch and Byram, 1968) and the Canadian Forest Fire Weather Index (FWI) (Flannigan et al., 1998). The KBDI is extensively used in the U.S. It is in essence an indicator of a deficit in soil moisture, which is assumed to saturate at a water depth equivalent of 20 cm. It is based on a number of physical assumptions. Soil water transfer to the atmosphere through evapotranspiration is determined by air temperature and annual precipitation which is used as a surrogate for the vegetation cover (areas with higher annual rainfall are assumed to support more vegetation). With higher values of the KBDI, fire becomes more intense due to an increased flammability of soil organic material and burned area becomes larger and period becomes longer due to fast spread of fire.

Another technique is to relate fire potential to fuel moisture. Fuel moisture can be calculated using models of varied complexity. Fosberg (1970) developed moisture diffusion models for fine fuels based on a time-lag property. Nelson (2000) developed a physical model to predict fuel moisture by describing processes for heat transfer and moisture movement within a wooden cylinder as well as between the atmosphere and the surface of the cylinder. Fuel moisture can also be detected using remote sensing from space (Verbesselt et al., 2003). Empirical methods have been used to obtain a correlation between fuel moisture and vegetation greenness indices such as the normalized difference vegetation index (NDVI) or its variations (e.g. Burgan and Hartford, 1997; Chuvieco et al., 2002; Dasgupta et al., 2007) and surface temperature (Jackson, 1986). More physically based methods have been developed to obtain fuel moisture using the inversion of coupled leaf and canopy radiative transfer models (Jacquemoud, 1993).

Regional climate modeling is a new technique for estimating fire potential over large areas that provides simulated and projected precipitation, air temperature, humidity, and winds for calculation of fire indices. Regional climate models (RCMs) have been developed to partially solve the problems associated with low resolution of three-dimensional general circulation models (GCMs) such as their inability to capture the mesoscale systems responsible for convective precipitation events. The effects of local and regional forcing such as spatial land-cover variability are often not well represented in GCMs. RCMs, on the other hand, have spatial resolution at tens of kilometers or higher and are often equipped with more detailed schemes for land surface and other local and regional processes, thereby providing a better tool for understanding climate at regional scale.

The inclusion of these local and regional processes provides RCMs with an advantage when applied to projecting future fire potential. Many GCMs have projected the overall drying trend in middle latitudes by the end of this century due to the greenhouse effect. Thus, it is likely wildfires will increase in many regions, as indicated in a recent study (Liu et al., 2009) that examined changes in KBDI produced by the climate change projected by HadCM3 with the A2a scenario and analyzed trends in global wildfire potential. RCMs can obtain high-resolution climate change with the present and future lateral boundary conditions provided by GCMs which allows RCMs to more precisely identify specific regions that will be impacted and the magnitude of those impacts. Moriando et al. (2006) used the output of the Hadley Centre Regional Circulation Model to calculate the FWI for the present and future Intergovernmental Panel on Climate Change (IPCC)'s climate scenarios.

RCMs include soil and vegetation schemes coupled with the atmospheric processes. These schemes use energy and water conservation equations to predict variations of soil moisture and other soil and vegetation properties. Since the KBDI is a measure of soil water deficit, it is equivalent to soil moisture anomalies. Thus, the projected soil moisture has the potential to be a direct measure of wildfire occurrence, although the actual value of this potential has yet to be assessed.

This study examines the ability of an RCM to evaluate fire potential during a drought event in the northern United States. The RCM was used to simulate atmospheric and soil conditions of a summer month in 1988, when the most severe drought of the past century occurred in the northern U.S. For comparison, a summer month of a number of other years, including 1993 when a severe flood event happened in the northern U.S., was also simulated. Fire potential was evaluated using both the KBDI, which was calculated based on the simulated atmospheric conditions, and soil moisture. Satellite remotely sensed data were used to evaluate the RCM simulations of soil moisture conditions. The research methods are described in Section 2. The results are presented Section 3, and conclusions and discussion are given in Section 4.

2. Methods

2.1. Regional climate modeling

The National Center for Atmospheric Research (NCAR) regional climate model (RegCM) (Giorgi et al., 1993a, 1993b) with modified explicit rainfall calculation (Giorgi and Shields, 1999) was used to conduct the regional climate modeling. RegCM characterizes regional features of climate by incorporating Biosphere–Atmosphere Transfer Scheme (BATS) land-surface physics (Dickinson et al., 1993) and the NCAR radiative transfer model (Kiehl et al., 1996) into the standard NCAR/Penn State Mesoscale Model (Anthes et al., 1987). RegCM is able to reproduce some important high-resolution spatial characteristics of climate for major geographic regions over the world.

BATS has three soil layers of the surface, root zone, and a third layer between the root zone and the groundwater layer. They extend from the soil surface to 0.1 m, 1 to 2 m (depending upon land-cover type), and 3 m, respectively. Soil moisture of each layer varies mainly as a result of precipitation, evapotranspiration, and runoff. Soil moisture is also determined by soil–vegetation water exchanges through root absorption in the root zone and water exchange with the groundwater layer in the third layer. The water level of the groundwater layer is assumed to be constant. Note that the water level could fluctuate remarkably during a prolonged drought event such as the 2003 European drought (Andersen et al., 2005).

The simulation periods are the July months during 1988 through 1995. The simulation domain covers the continental U.S. and parts of Canada and Mexico (Fig. 1). The topography is characterized by mountains in the west and flat lands in the east. The dominant land-cover types include coniferous forest and grass in the Northwest, coniferous forest, grass, and desert in the Southwest, agriculture in the Midwest, deciduous forest in the Northeast, and mixed forest, wet land and agriculture in the Southeast. The domain is centered at 40°N and 99°W and contains 97 by 61 grid points with a horizontal resolution of 60 km. There are 14 vertical layers with the top model atmosphere at 80 hPa. The Grell sub-grid convective scheme (Grell et al., 1994) was utilized.

The initial and horizontal lateral boundary conditions for the RegCM simulations of wind, temperature, water vapor, and surface pressure were interpolated from the analysis of the European Center for Medium-Range Weather Forecast (ECMWF), which has a resolution of 1.875° of latitude and longitude (roughly 200 by 175 km at mid-latitudes). Soil water content was initialized as described in Giorgi and Bates (1989), i.e., the initial soil moisture content is equal to the sum of wilting soil moisture, at which transpiration ceases, and the difference between saturation and wilting soil moisture weighted by the soil moisture availability, which is specified for each surface type. Time dependent sea-surface temperature (SST) was interpolated from a set of observed, monthly mean with a resolution of 1° (Shea et al., 1992). The meteorological and SST data were obtained from the archives of the NCAR Scientific Computing Division. Land type was specified based on the global

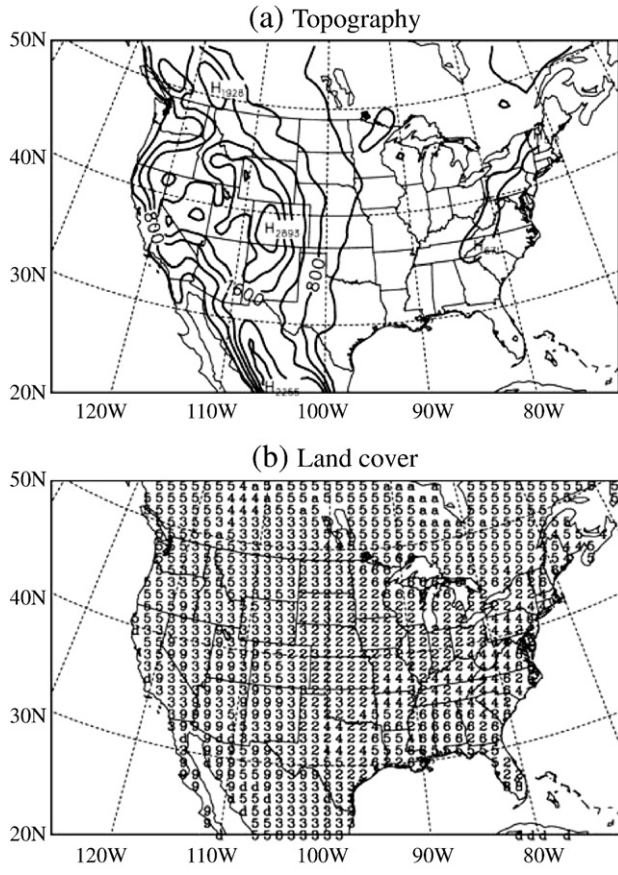


Fig. 1. Simulation domain. (a) Topography with contour interval of 400 m. (b) Land cover with legend shown below the figure.

1-km resolution International Geosphere Biosphere Program (IGBP) land-cover dataset (Zeng et al., 2000). All data were converted to the RegCM resolution of 60 km using double linear interpolation for ECMWF meteorology and SST and using dominant vegetation type within a RegCM grid cell.

There are a number of limitations with the RCM modeling technique (Liu, 2007). First of all, RCMs are driven by GCMs and/or measurements and any errors in lateral conditions will be passed to RCMs. Experiments have indicated large sensitivity of RCM simulations to lateral conditions. Even though complex local land-surface conditions were one of the reasons for using RCMs, information deficiencies limit the ability of RCMs to reproduce important features in the atmosphere and other earth components. In addition, domain size and internal variability created by disturbances in initial and boundary conditions also affect RCM performance (Seth and Giorgi, 1998; Giorgi and Bi, 2000).

2.2. KBDI

The KBDI is calculated using

$$Q = Q_0 + dQ - dP, \quad (1)$$

$$dQ = 10^{-3}(800-Q)(0.968e^{0.0486T}-8.3)d\tau / (1 + 10.88e^{-0.0441R}), \quad (2)$$

where Q and Q_0 are the moisture deficiency (KBDI) of current and previous day, respectively, dQ is the KBDI incremental rate, T is the daily maximum temperature at 2 m above the ground, dP is daily

precipitation, R is the mean annual rainfall, and $d\tau$ is a time increment set equal to one day. Note that $dQ=0$ when $T \leq 50^\circ\text{F}$ (10°C) and only the portion of daily precipitation above the net accumulated precipitation of 0.5 cm (0.20 in.) is used. The KBDI value ranges between 0 and 800. The initial KBDI values were determined based on relative root-layer soil moisture on the first simulation day of each year. Soil moisture percentage ranges between 0 and 100, with 100 representing saturated soil. A factor of 8 was applied to the percentage so that the range now is between 0 and 800. The initial KBDI is the difference between 800 and the modified percentage. Wildfire potential is divided into four levels based on KBDI values: low (KBDI below 200), moderate (200–400), high (400–600), and extreme potential (above 600).

The KBDI was formulated under the climate conditions in the southeastern U.S. Direct comparison of specific KBDI values for locations with different climate is often problematic as the drying rate in the index is a function of the mean annual precipitation for a location. Because the index was developed for the southeastern U.S., the exact functional form of this relationship may not be valid for annual rainfall amounts that differ significantly from those of this region as was shown by Snyder et al. (2006) for arid grasslands in California; however the KBDI still maintained respectable agreement with volumetric soil water content. Xanthopoulos et al. (2006) found that the KBDI reasonably reflected cumulative moisture deficits in the duff and upper soil layers in the vicinity of Athens, Greece, and also reflected to some extent water deficit in living plants and their potential flammability. Despite the potential limitations of the functional form used in the KBDI to parameterize evapotranspiration, the index is still a viable means of assessing the potential impacts of a changing climate on fire potential by focusing on the relative changes in KBDI produced by changes in temperature and precipitation.

2.3. Historical wildfire

The fire data were prepared by the U.S. Bureau of Land Management (BLM, 2003) fire information system. The fire parameters include size (in acres), number, location (states or regions), types (wildfire suppression, natural outs, support actions, prescribed fire, and false alarm), causes, and agency (BLM, Bureau of Indian Affairs, Fish and Wildlife Service, National Park Service, and USDA Forest Service). The data used for this study are monthly totals of area burnt by wildfires by state (the 48 contiguous states). Wildfires are comprised of the fire types of wildfire suppression and natural outs.

2.4. Evaluation of soil moisture simulation with NDVI

Soil moisture is one of the simulated meteorological and soil properties used for wildfire potential evaluation. Unlike other properties (i.e., precipitation and air temperature), no soil moisture measurements are available for its simulation. Because vegetation conditions are closely related to soil moisture at monthly or longer scales, we used a vegetation index based on satellite remotely sensed data, the NDVI (Tucker, 1979), to evaluate the simulated soil moisture anomalies. The 10-day composite NDVI images for July 1988 and 1993 prepared by the National Aeronautics and Space Administration (NASA) were used in this study.

NDVI is the difference in the spectral reflectance between the near-infrared and visual wavelengths divided by their sum. Most types of vegetation strongly absorb photosynthetically active radiation and weakly absorb near-infrared radiation, resulting in small and large reflectance, respectively. Clouds, meanwhile, have the opposite reflectance dependence in the two spectral regions. Thus, NDVI can be used to indicate vegetation and its conditions. NDVI ranges between -1 and $+1$ with the two ends for water and forest, respectively, around 0 for sand and rocks, and about 0.2 to 0.4 for grass and shrub. The advantages of NDVI data for monitoring vegetation change include

complete spatial coverage of earth surfaces, temporal coverage at regular intervals, and a landscape-scale signal that includes current status of all plant species on site. The disadvantages of using NDVI are loss of data due to cloud cover, effects of non-vegetated surfaces, calibration issues between satellites and between sensors, and the complexity of interpreting the data (Huete, 1988).

3. Results

3.1. Simulated drought and flood events

3.1.1. Precipitation

Fig. 2 shows the simulated July precipitation for the 8-year average and anomalies in 1988 and 1993. For the average, large precipitation occurred in the Atlantic coast with peak monthly rainfall of 280 mm found in the Southeast. The North American planetary-scale westerly trough was located along the eastern coast, which is a main contributor to the large rainfall in this area. Precipitation gradually decreased westward. The smallest monthly rainfall of about 40 mm was found along the Pacific coast, where most precipitation occurs in winter instead of summer.

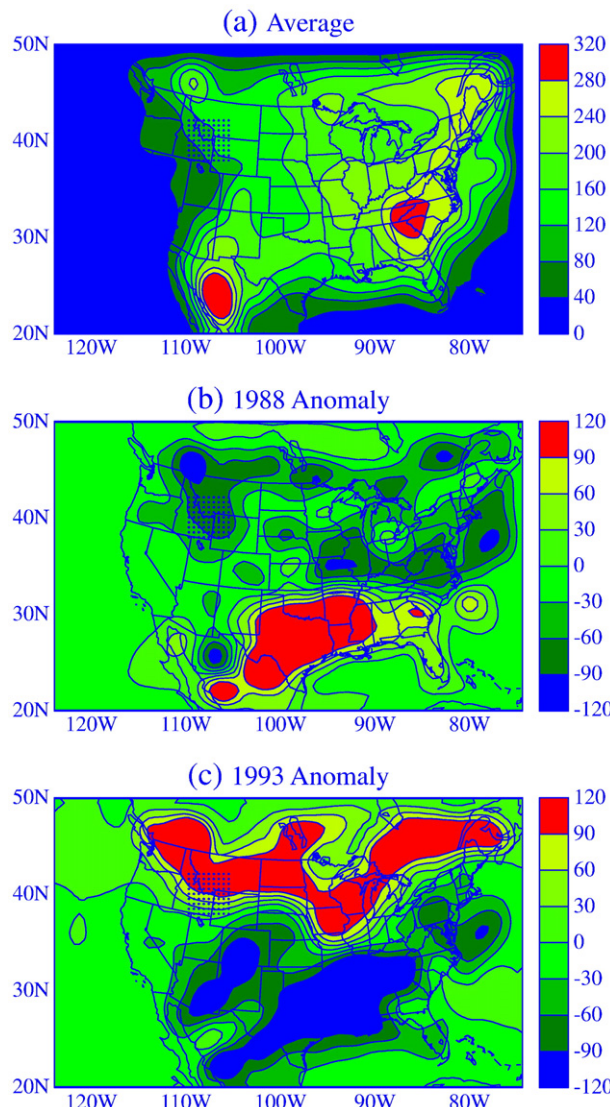


Fig. 2. Simulated July precipitation with RegCM (in mm) for 8-year average (a), anomaly in 1988 (b), and anomaly in 1993 (c). The dot area indicates the 1988 Fire Region.

The spatial pattern of the July 1988 anomalies was characterized by the overall decrease in precipitation in the northern U.S. and increase in the southern U.S. The monthly rainfall decrease of 60 mm was found in two regions of the northern Rocky Mountains and the area from the southern Midwest to middle Atlantic coast. Rainfall was well above the average in the area from Texas to the southern Atlantic coast. The spatial pattern of the July 1993 anomalies, on the other hand, was opposite to that of 1988 and characterized by overall rainfall increase in the northern U.S. The positive anomalies of monthly rainfall over 90 mm were found in the Midwest. In contrast, rainfall in most of the southern U.S. was below average.

Meteorological conditions were averaged over a northern Rocky Mountain region to obtain conditions related to the severe 1988 wildfires, including the Yellowstone National Park wildfire (Romme and Despain, 1989). This region, denoted as "1988 Fire Region" hereafter, comprises an area of $480 \times 480 \text{ km}^2$ within the states of Wyoming, Montana and Idaho and includes Yellowstone National Park. The July 1988 rainfall of this region was 36 mm, a decrease of 66 mm (65%) from the 8-year average of 102 mm (Table 1). In contrast, the amount for 1993 was 177 mm, 74% (75 mm) higher than average.

The simulated spatial pattern of average precipitation is the same as the observed pattern (Fig. 3). The magnitude of rainfall, however, is over-predicted in the eastern U.S. Also the largest rainfall in the Southeast is located farther north in the simulation than observed. This shift is probably related to the lateral boundary issue of regional climate modeling. More water vapor in the atmosphere may be transported into the interior of the simulation domain instead of staying in the boundary areas. The spatial pattern of the simulated low (large) July precipitation in 1988 (1993) in the northern U.S. agreed with the observed pattern at the continental scale despite the larger magnitude of the simulated anomalies. However, spatial patterns differed at the regional scale. For example, the precipitation decrease in July 1988 was found in the northern Rocky Mountains in the simulated instead of the northern Midwest as was seen in the observed rainfall.

The simulated precipitation anomalies in the northern U.S. represent the conditions during the prolonged 1988 drought and 1993 flood events in this region, two of the most severe weather extremes in the 20th century. In 1988, precipitation was lower than the average in late April and reached the greatest deficiencies in June. This period was among the driest of the past century in the continental U.S. (Karl et al., 1988). By July precipitation returned to normal in some northern U.S. regions, but was still well below normal in the northern Midwest and eastern Northwest, where monthly rainfall was less than 75 mm. During June through August 1993, on the other hand, rainfall totals were from 300 to 1000 mm across these areas. The amounts were approximately 200–350% of normal from the northern Great Plains southeastward into the central U.S.

3.1.2. Temperature

Fig. 4 shows the simulated July maximum surface air temperature near the ground for the 8-year average and anomalies in 1988 and

Table 1

Simulated precipitation (P), maximum temperature (T_{\max}), surface-layer and root-layer soil moisture (S_{sw} and S_{rw}), evapotranspiration (E), and runoff (R) averaged over the 1988 Fire Region (see text for the location of this region).

	Average	1988			1993		
		Value	Diff	Rate (%)	Value	Diff	Rate (%)
P (mm/mon)	102	36	-66	-65	177	75	74
T_{\max} (°C)	26.7	28.5	1.8		21.2	-5.5	
S_{sw} (mm)	20.5	16.7	-3.8	-18.5	24.8	4.3	21.0
S_{rw} (mm)	328	312	-16	-4.9	352	24	7.3
E (mm/mon)	105	84	-21	-20	102	-3	-2.9
R (mm/mon)	13	2	-11	-85	34	21	162

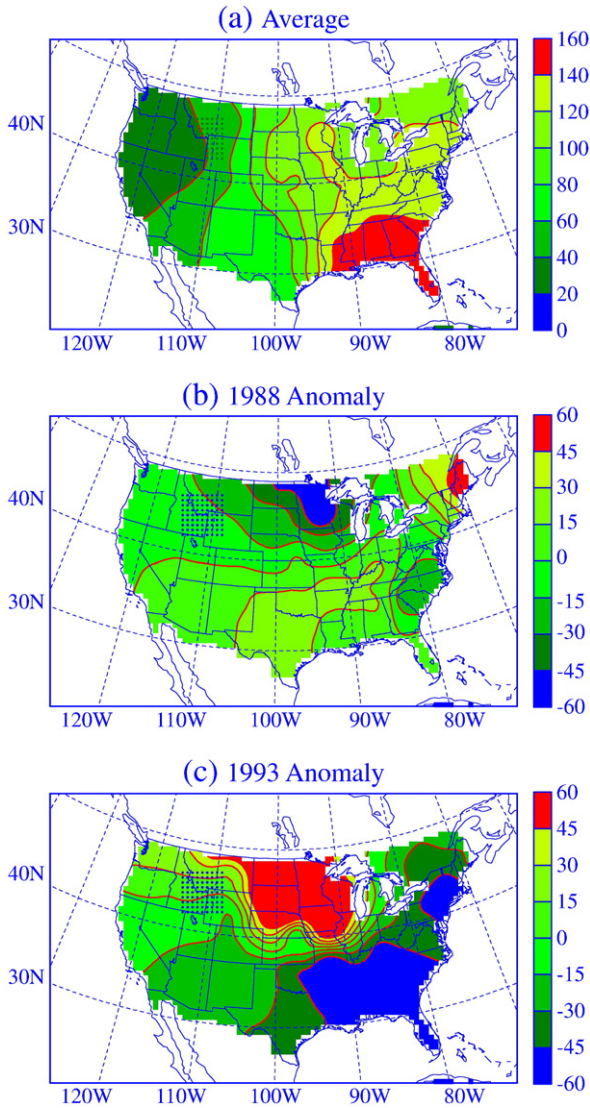


Fig. 3. Same as Fig. 2 except for observed precipitation.

1993. Note that maximum air temperature rather than average air temperature is displayed because the KBDI calculation uses the maximum air temperature. The temperature average generally decreased from over 35 °C in the southern U.S. to about 20 °C in the northern U.S., reflecting the latitudinal dependence of solar radiation. Two warm tongues extended from Texas to the northern Great Plains and along the Pacific coast. They were separated by the Rocky Mountains, where temperature was lower due to the high elevation. Temperature was lower along the Atlantic coast, coincident with the peak in rainfall, than the central U.S. at the same latitudes, an indication of the effect of clouds and precipitation.

The air temperature anomalies in July 1988 were positive in the northern U.S. An increase of 2 °C was found from the middle Pacific coast to the northern Rocky Mountains and into the northern Great Plains. In contrast, the anomalies were negative in the southern U.S., with -2°C found in Texas. Similar to precipitation, the spatial pattern of July air temperature anomalies in 1993 was opposite to that in 1988: the anomalies were negative in the Northwest and positive in the Southeast with a magnitude of 3 °C. The temperature anomaly for the 1988 Fire Region was 1.8 °C in 1988 and -5.5°C in 1993 (Table 1).

The observed July surface air temperature near the ground (Fig. 5) had the same spatial pattern as the simulated temperatures, showing the northwardly decreasing trend, two warm tongues, and the

difference between the Atlantic coast and the central U.S. The simulated July temperatures were abnormally hot in 1988 and cool in 1993 in the northern U.S., which was seen in the observed temperatures as well. The amplitudes of the simulated maximum air temperature anomalies, however, were almost twice those of the observed air temperature anomalies.

The above results suggest that the model reproduced some basic features of the 1988 drought and 1993 flood events in the northern U.S. during the month of July. The spatial patterns of air temperature anomalies matched those of precipitation, that is, drier and hotter in the northern (southern) and wetter and cooler in the southern (northern) U.S. in 1988 (1993). Physically, less precipitation (or clouds) means less solar radiation reflected back into space and therefore more solar radiation absorbed by the ground; this leads to larger sensible heat flux from the ground into the atmosphere and therefore higher air temperature. Furthermore, less precipitation in a large geographic area is related to abnormally intense anti-cyclonic atmospheric circulation systems that bring stable stratification and subsiding airflow leading to heating of the air near the ground. However, the location and extent of hotter (cooler) areas did not match exactly those of drier (wetter) areas. Besides clouds, temperature at a location is also affected

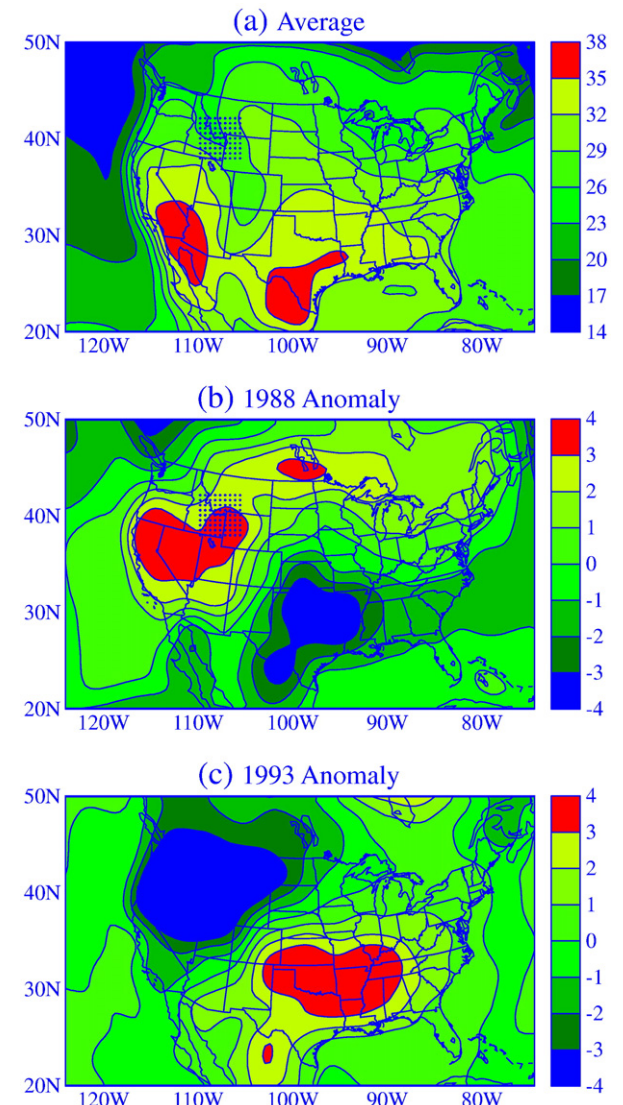


Fig. 4. Simulated July maximum air temperature near the ground with RegCM (in °C) for 8-year average (a), anomaly in 1988 (b), and anomaly in 1993 (c).

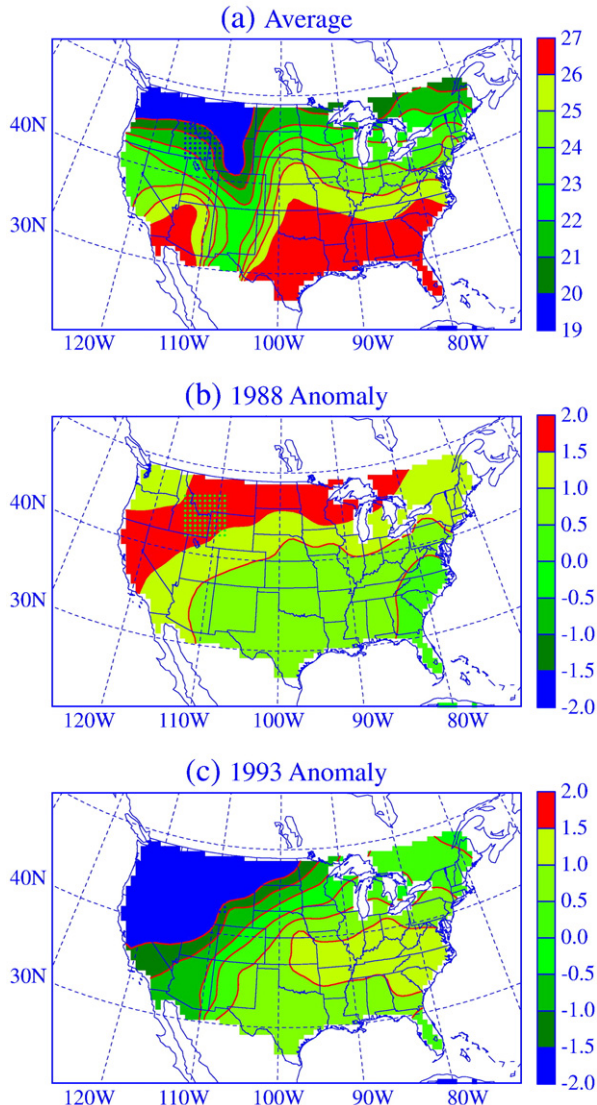


Fig. 5. Same as Fig. 4 except for observed air temperature.

by other factors such as horizontal heat transport and evapotranspiration on the ground.

3.2. Evaluation of fire potential using KBDI

Fig. 6 shows the 8-year average KBDI and anomalies in 1988 and 1993. The KBDI average generally decreased from the southwestern U.S. to northeastern U.S. The largest KBDI of more than 400 (high fire potential) was found in the Inter-mountains, the driest areas in the U.S., and central Rocky Mountains. The KBDI was between 200 and 400 (moderate potential) in the northern and southern Rocky Mountains, and below 200 (low potential) in the rest of the continental U.S.

The KBDI in July 1988 increased in the northern U.S. The largest increase of more than 200 units was found in the northern Rocky Mountains. The KBDI in the 1988 Fire Region was 444, an increase by 193 units (77%) from the 8-year average of 251 (Table 2). The fire potential therefore was upgraded from moderate for the average condition to high for 1988. In contrast, the KBDI decreased in the southern U.S. The spatial pattern of the KBDI anomalies in July 1993 was opposite to that in 1988. The KBDI decreased in the northern U.S. and increased in the southern U.S. The magnitude of 200 units was found in the northern Rocky Mountains and the western Southeast. The KBDI in the 1988 Fire Region was 166, a decrease by 85 units

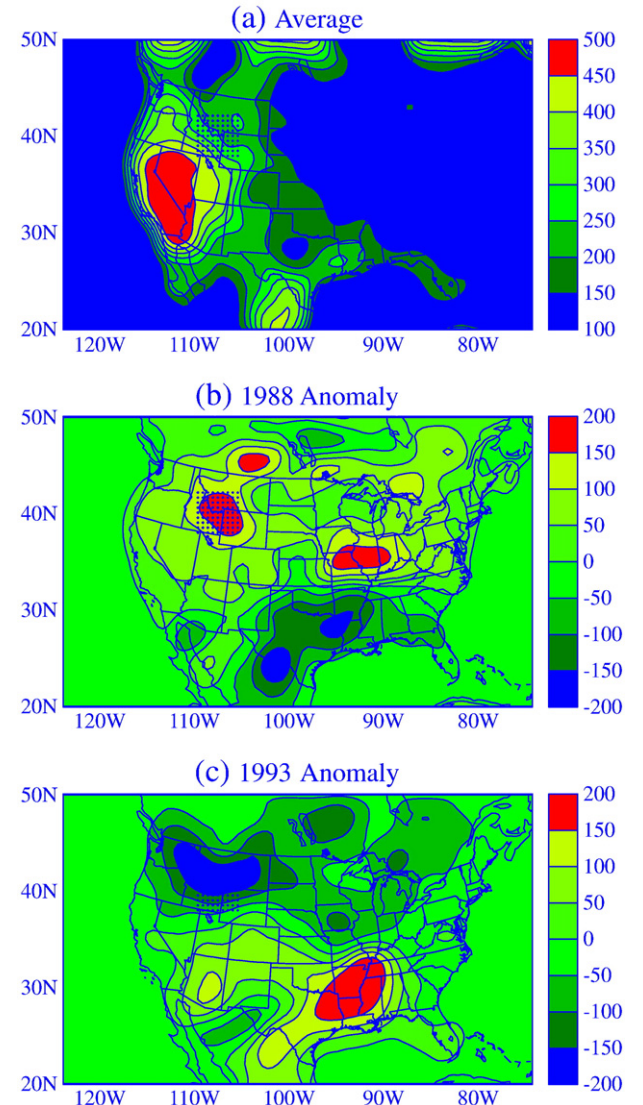


Fig. 6. The July Keetch-Byram Drought Index calculated using the simulated precipitation and maximum air temperature with RegCM (in mm) for 8-year average (a), anomaly in 1988 (b), and anomaly in 1993 (c).

(34%) from the 8-year average (Table 2). The fire potential therefore was downgraded from the moderate average condition to low for 1993.

According to the guidelines on expected fire conditions and potential suppression problems for various ranges of the KBDI for the southeastern U.S. (Melton 1989), when fire potential is high, especially when the KBDI exceeds 500, wildfires become much more intense. Also suppression/control of fires becomes increasingly difficult, which generally results in larger fire sizes. The upgrade of fire potential from moderate to high level in the 1988 Fire Region suggests

Table 2

KBDI averaged over the 1988 Fire Region. P and T represent precipitation and maximum air temperature, respectively. ΔKBDI is the difference in KBDI between a specific year and the 8-year average.

Year	Anomalies in		None P or T		Both P and T		P only		T only	
	Average		1988	1993	1988	1993	1988	1993	1988	1993
KBDI	251		444	166	436	175	293	232		
ΔKBDI	0		193	-85	185	-76	42	-19		
%	0		77	-34	74	-30	17	-8		

that the occurrence of intense and extensive wildfires should be very likely under the drought condition.

The actual July wildfire occurrence (Fig. 7) provides evidence for the KBDI evaluation of fire potential. To obtain the spatial distribution of wildfires, an interpolation technique (Englisch, 1968) was used to convert the burned areas of individual states to the RegCM domain of 97×61 grid points. This technique applies a weight factor, which is inversely proportional to the distance between a grid point and a state. The 8-year average of burned area was the largest in the Northwest, with the value more than 500 acres burned/1000 km 2 found in the northern Rocky Mountains. The burned area was between 2 and 5 acres burned/1000 km 2 in the Southwest and less than 2 acres burned/1000 km 2 east of the Rocky Mountains. The intermountain region had small actual burned area despite the high fire potential because a majority of the region is covered with bare ground or low productivity vegetation, thus lacking in sufficient fuels. Note that the burned area dataset was collected only on federal lands and thus underestimates the area burned in the eastern U.S. where private and state land ownerships predominate.

The 1988 severe wildfires in Yellowstone National Park and the rest of the northern Rocky Mountains resulted in a huge burned area. The largest value was more than 2500 acres burned/1000 km 2 , about

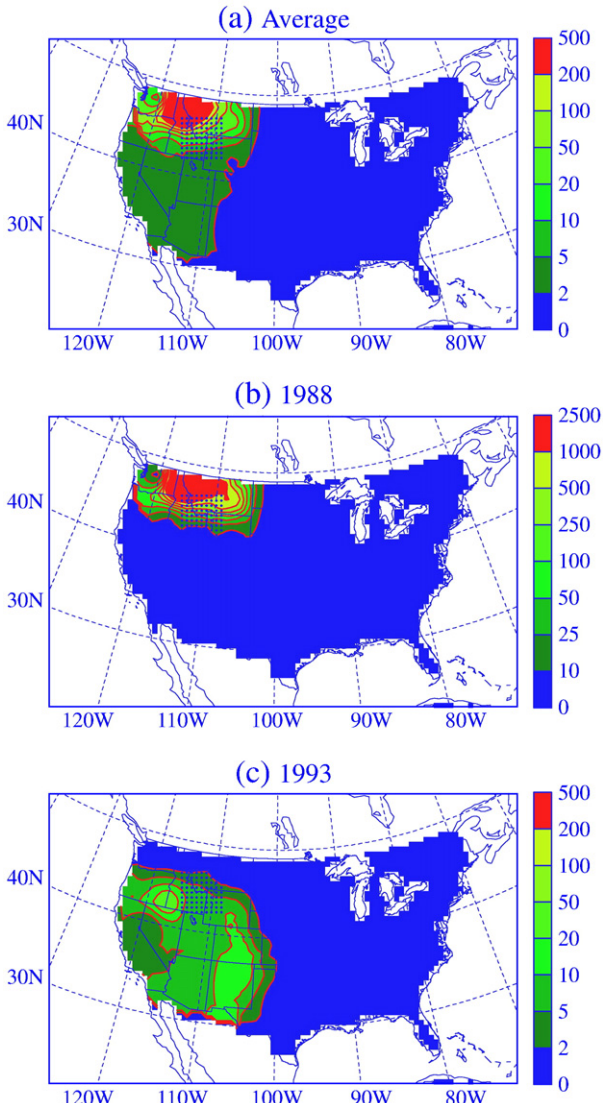


Fig. 7. July burned area on federal lands by wildfires (in acres burned/1000 km 2). Panels (a) to (c) are 8-year average, 1988, and 1993.

5 times of the average. In 1993, on the other hand, burned area was less than 2 acres burned/1000 km 2 in this region. But burned area in the Southwest increased by up to 20 acres burned/1000 km 2 .

To examine the relative importance of precipitation and maximum air temperature, two more KBDI calculations were made for 1988 and 1993, each with only precipitation or temperature anomalies. With only precipitation anomalies, KBDIs was 436 for 1988 and 175 for 1993, changing by 185 (74%) and -76 (-30%), respectively, from the average (Table 2). The corresponding KBDI with only temperature anomalies was 293 and 232, changing by 42 (17%) and -19 (-8%). The magnitude of the KBDI change due to the precipitation anomalies was about 4 times that due to the temperature anomalies alone. Thus, precipitation anomalies are a dominant contributor to the change in KBDI.

Note that the initial KBDI was assigned based on the root-layer soil moisture. Because soil moisture is not routinely measured by weather stations, the initial soil moisture conditions have to be specified by using empirical methods or assimilation techniques. This is one of the major uncertainties in RCM simulations and it is passed over to the calculation of the KBDI. This uncertainty, however, only affects the absolute value of the KBDI, not the difference between an individual year and the average. Thus, although a different initial soil moisture would have produced a different KBDI for 1988 (that is, 444 as shown in Table 2), the change from the average would have been the same (193).

3.3. Evaluation of fire potential using simulated soil moisture

Fig. 8 shows the simulated July surface-layer soil moisture for the 8-year average and anomalies in 1988 and 1993. Soil moisture average ranged between 16 and 32 mm, generally increasing from the Pacific to Atlantic coast. This was similar to the spatial pattern of average precipitation. Unlike rainfall, which was the largest along the Atlantic coast, however, soil moisture was the largest in the northern Midwest. This was due to the relatively low temperature and therefore low evapotranspiration.

The simulated drought in 1988 resulted in large water stress in the northern Rocky Mountains, where soil moisture was 8 mm (30%) lower than the average. Large reductions in soil moisture were also found in the area from the southern Midwest to the middle Atlantic coastal region. In contrast, soil moisture increased by 8 mm in Texas. In 1993, soil moisture increased in the northern U.S. and decreased in the southern U.S. The anomalous spatial patterns of surface-layer soil moisture in 1988 and 1993 were similar to the corresponding precipitation patterns. The surface-layer soil moisture for the 1988 Fire Region was reduced by 3.8 mm (18.5%) from the average of 20.5 mm in 1988 and increased by 4.3 mm (21%) in 1993 (Table 1).

For the root layer (Fig. 9), the soil moisture average was the largest along the Atlantic coast and smallest along the Pacific coast, with values of 600 and 200 mm, respectively. Despite the general similarity in spatial pattern, the root-layer soil moisture differed noticeably in two ways from precipitation. First, soil moisture was the smallest in the central and southern Rocky Mountains and Intermountain West instead of the Pacific coast. It gradually increased toward the northern Rocky Mountains. Second, there was another region of high soil moisture values in the northern Midwest in addition to the one along the Atlantic coast. The spatial patterns of the root-layer soil moisture anomalies differed little from the patterns of surface-layer soil moisture. The root-layer soil moisture for the 1988 Fire Region was reduced by 16 mm (4.9%) in 1988 from the average of 328 mm and increased by 24 mm above average (7.3%) in 1993 (Table 1).

The simulated soil moisture anomalies can be validated to a certain extent by comparing the July NDVI values between 1988 and 1993 (Fig. 10). For both years, most of the eastern U.S. had high values between 0.5 and 1, indicating vegetation under moist conditions, while most of the western U.S. had the values about 0.2, indicating

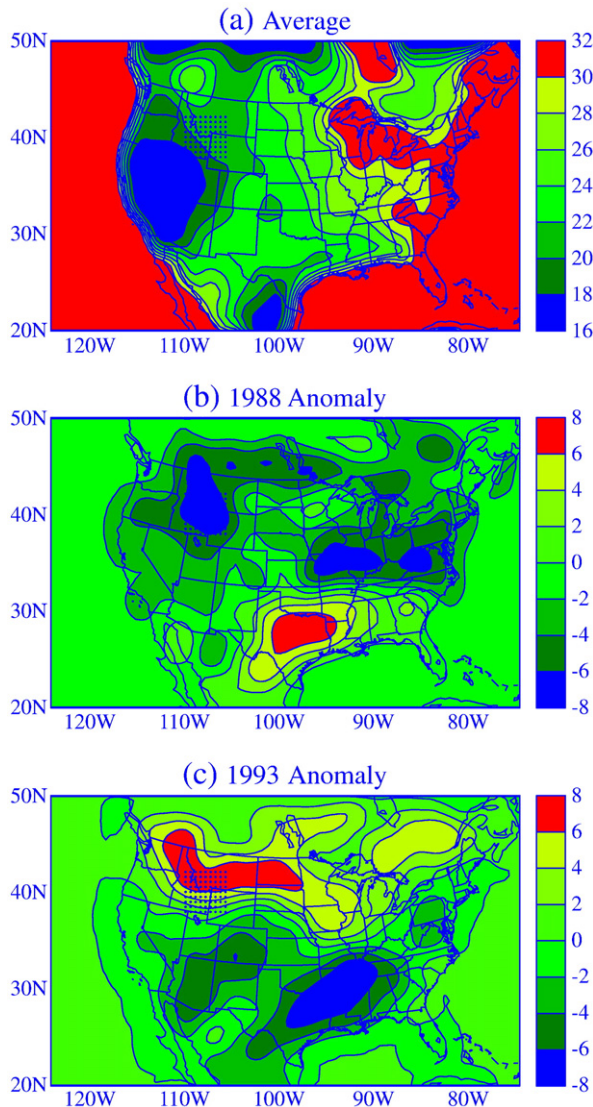


Fig. 8. Simulated July surface-layer soil moisture with RegCM (in mm) for 8-year average (a), anomaly in 1988 (b), and anomaly in 1993 (c).

vegetation under dry conditions. Some areas in the western U.S., especially the Southwest, had values around zero, indicating bare soil or extremely dry vegetation. The vegetation conditions changed during the course of each month in the two years. There were more spots with NDVI around zero in the northern Rocky Mountains in 1988 than 1993, especially for the second and third 10-day periods. This indicates drier vegetation and soil conditions in 1988.

The simulated soil moisture was reduced in 1988 in the 1988 Fire Region, indicating a certain degree of soil water deficit, which is consistent with a larger KBDI and therefore increased wildfire potential. However, the magnitude of the simulated root-layer soil moisture anomaly was just slightly more than 10 mm or about 5% of total soil moisture; this change was not significant enough to predict the abnormally intense and extensive wildfires. Thus, for the specific case examined in this study, the simulated soil moisture anomalies were not a good indicator for wildfire potential.

4. Conclusions and discussion

Regional climate models can be a useful tool for wildfire potential evaluation by either providing meteorological information for computing fire indices such as the KBDI, or predicting soil moisture anomalies which are roughly equivalent to the KBDI and therefore

could be a more direct measure of fire potential. These two roles of RCMs have been investigated in this study by examining the 1988 northern U.S. drought as well as other meteorological conditions using the NCAR regional climate model. The results provided supportive evidence for the value of the meteorological information in computing fire indices, but not for assessing fire potential from simulated soil moisture using current land-surface models.

The role of regional climate modeling in providing useful meteorological information for computing KBDI and evaluating fire potential has important implications for projection of future wildfire potential. The United States is one of the regions in the world where wildfires are projected to increase significantly under the changing climate projected by GCMs (Liu et al., 2009). The recent report on global climate change impacts in the United States (Karl et al., 2009) saw increased wildfires, especially in the West because of warmer and drier weather in the 21st century. The local climate change for this report was obtained from the GCM projections using statistical downscaling techniques developed based on historical climate data. An international research program, the North American Regional Climate Change Assessment Program (NARCCAP) (Mearns, 2010), is underway to produce high-resolution climate change simulations. It investigates uncertainties in regional scale projections of future climate and generates climate change scenarios for use in impacts

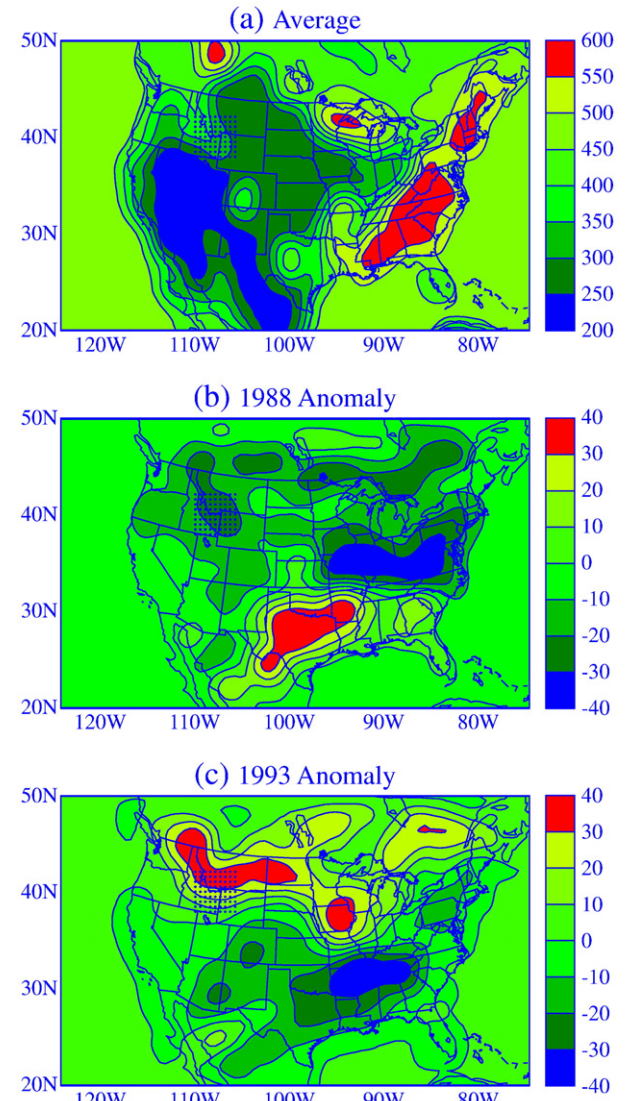


Fig. 9. Same as Fig. 8 except for the root-layer soil moisture.

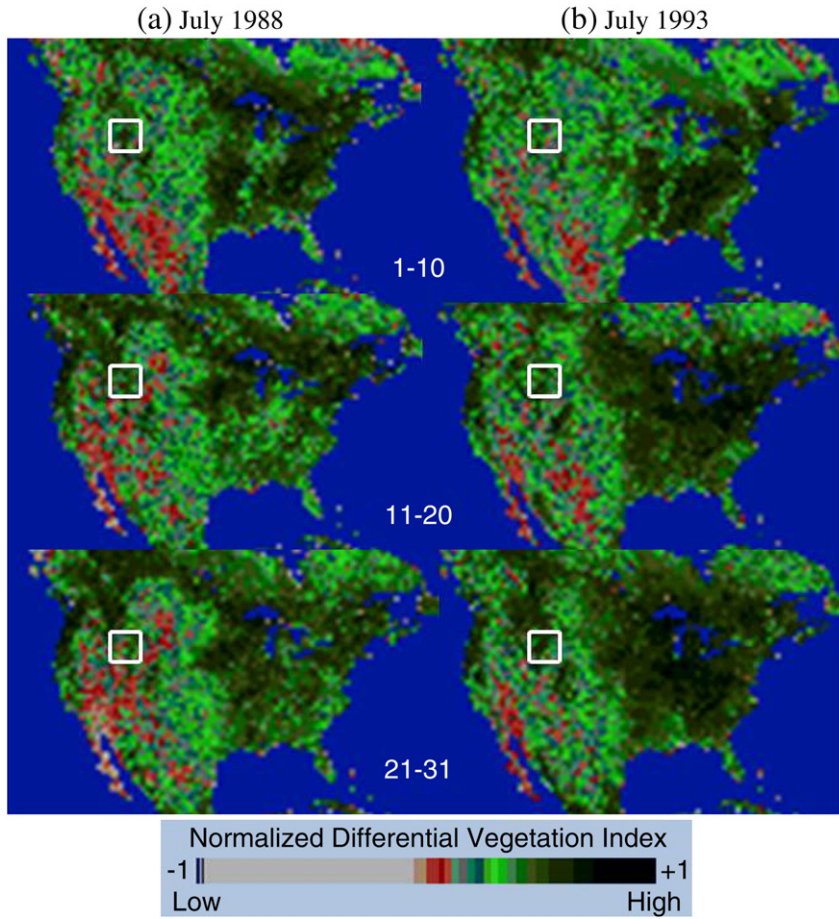


Fig. 10. July ten-day composite Normalized Differential Vegetation Index (NDVI) from the Advanced Very High Resolution Radiometer (AVHRR) for 1988 (top) and 1993 (bottom). The box indicates the 1988 Fire Region (produced by NASA).

research by running a set of RCMs driven by a set of GCMs. The more physically based downscaling data of precipitation and maximum air temperature projections are expected to improve future U.S. wildfire projections, among others, over the statistical downscaling techniques.

Another issue with the evaluation of this role is the specification of initial soil moisture, which is not a routine measurement parameter. It can be partially addressed by the application of remote sensing and assimilation of soil moisture. Recent technological advances in satellite remote sensing have shown that soil moisture can be measured by a variety of remote sensing techniques including optical, thermal, passive microwave, and active microwave measurements (Wang and Qu, 2009). The satellite remotely sensed vegetation condition was used to evaluate the soil moisture simulation in this study despite no direct application of remotely sensed soil moisture. The major concern with using remotely sensed data in fire potential applications is that only the surface soil moisture can be directly detected, while physically or empirically based relations have to be used to further obtain deep-layer soil moisture. Many soil moisture assimilation schemes have been developed, which provide improved initial conditions for regional models and help increase accuracy of monthly and seasonal predictions (Koster et al., 2010).

The role for regional climate modeling in predicting fire potential can be further explored by examining other fire indices that use different meteorological parameters than the KBDI. For example, the FWI considers the impacts of winds on wildfire ignition and spread in addition to precipitation and temperature. Wind is a meteorological field specifically affected by local topography due to both mechanical and thermal complexity (Linn et al., 2007), which are characteristics

of most of the western U.S. that is typically mountainous. The Santa Ana wind is an example of the complex interactions among topography, wind, and wildfire in the western U.S. The Santa Ana winds are the hot and warming airflows funneled toward passes in the southern California coastal ranges by the higher Sierra Nevada range and the Rocky Mountains and may exceed 30 m/s in extreme cases. They quickly reduce fuel moistures, greatly enhancing the risk of fire, and fan the flames of any fire once started (Westerling, 2004). The ability of GCMs to represent the impact of local topography is limited due to their low spatial resolution. Statistical downscaling techniques have additional sources of uncertainty due to the sparse meteorological observation network in mountain areas. With high spatial resolution, RCMs can better represent topography and produce more reasonable local winds. This is expected to significantly improve the calculation of FWI in the western U.S.

On the other hand, this specific drought case study did not provide sufficient evidence for direct application of simulated soil moisture to evaluate wildfire potential. Many factors could contribute to this. First of all, the ecosystems in drier areas have the capacity to conserve moisture. Drought reduces the amount of water reaching the soil. Under persistent dry atmospheric conditions, however, plant stomata close to conserve stored water, reducing the transfer of soil water to the atmosphere through root absorption and transpiration (McDowell et al., 2008). Furthermore, runoff is reduced as a result of reduced precipitation. These changes will offset some of the impact of the reduced precipitation. As shown in Table 1, the simulated July evapotranspiration ranged from 105 mm for the average to 84 mm for 1988 at the 1988 Fire Region, a reduction by 21 mm (20%). The corresponding runoff changed from 13 to 2 mm, a reduction by

11 mm (85%). Note that the sum of the reductions in evapotranspiration and runoff was –32 mm, which accounted for only about half the reduction in precipitation of –66 mm. Reductions in other water exchange processes should have accounted for the rest of the reduction in precipitation. Infiltration and percolation to ground water were expected to decrease because of smaller soil moisture. Interception of precipitation by vegetation was also expected to decrease because of smaller leaf area index under drying conditions. Note that the changes in soil water exchanges for the flood event in 1993 were not always opposite to those for the drought event in 1988. The evapotranspiration actually decreased as well because of the reduced temperature. Also note that, although plant transpiration via stomata decreases, the guttation via leaf tooth glands increases (particularly among sclerophyll taxa like some *Ilex* species) in order to maintain “normal” sap flows into xylem vessels. Thus the evapotranspiration component due to plants could be approximately the same as in non-cold conditions in certain ecosystems.

Secondly, temporal variations in soil moisture are slower than those in the atmosphere. The variations of the air temperature and precipitation are significant at short scales such as daily and weekly. Soil moisture of the surface layer is determined by the direct interactions with the atmosphere through water exchanges (precipitation and evapotranspiration). Thus, it basically responds to the atmospheric variations. For example, the magnitude of the simulated surface-layer soil moisture decreased in 1988 was 3.8 mm (Table 1), representing a rate nearly 4 times of that of the root layer. Soil moisture of the root layer, however, varies at monthly or longer time scales mainly due to its capacity to buffer changes. Thus, soil moisture does not respond fully to the persistent atmospheric dry conditions over a short period (one month for this study).

Thirdly, soil moisture simulation has many uncertainties. The simulation depends on the initial condition, which was specified based on soil- and land-cover type and therefore independent of time in this study. This assumes no difference in initial soil moisture condition between a normal year and a drought or flood year. This was unlikely. Furthermore, soil moisture interacts with groundwater layer, especially the level of the water table which likely varies with antecedent moisture and current recharge from precipitation. In the 2003 drought in Europe, for example, groundwater levels varied considerably (Andersen et al., 2005). This important mechanism has been incorporated into land-surface schemes recently (Anyah et al., 2008); however, it was not an option for the BATS scheme used for this study. In addition, BATS may be somewhat insensitive when simulating soil moisture variation under dry conditions. Soil moisture data and model experiments are needed to further investigate this aspect of BATS, which is beyond the scope of this study. Clearly more investigations of drought conditions are needed, along with longer model integration periods, different RCMs, sensitivity experiments and evaluations of soil moisture simulations with various land-surface models under drought stress, in order to provide a more complete understanding of the use of RCM for fire potential modeling.

Acknowledgements

This study was supported by the USDA Forest Service. The meteorological data for driving the regional climate model were obtained from the National Center for Atmospheric Research. We would like to thank the editor and two anonymous reviewers for their insightful comments that helped improve the manuscript.

References

- Ackerman, A.S., Toon, O.B., Stevens, D.E., Heyms, A.J., Ramanathan, V., Welton, E.J., 2000. Reduction of tropical cloudiness by soot. *Science* 288, 1042–1047.
- Amiro, B.D., Todd, J.B., Wotton, B.M., 2001. Direct carbon emissions from Canadian forest fires. *Canadian Journal of Forest Research* 31, 512–525.
- Andersen, O.B., Seneviratne, S.I., Hinderer, J., Viterbo, P., 2005. GRACE-derived terrestrial water storage depletion associated with the 2003 European heat wave. *Geophysical Research Letters* 32 (L18405). doi:10.1029/2005GL023574.
- Anthes, R.A., Hsie, E.-Y., Kuo, Y.-H., 1987. Description of the Penn State/NCAR Mesoscale Model Version 4 (MM4), Technical Note, NCAR/TN-282+STR. National Center for Atmospheric Research, Boulder, Colorado. 66 pp.
- Anyah, R., Weaver, C.P., Miguez-Macho, G., Fan, Y., Robock, A., 2008. Incorporating water table dynamics in climate modeling: 3. Simulated groundwater influence on coupled land-atmosphere variability. *Journal of Geophysical Research* 113, D07103. doi:10.1029/2007JD009087.
- BLM (U.S. Department of Interior Bureau of Land Management), 2003. Federal Fire History Internet Map Service User Guide. www.firehistory.blm.gov.
- Burgan, R.E., Hartford, R.A., 1997. Live vegetation moisture calculated from NDVI and used in fire danger rating. In: Greenlee, Jason (Ed.), 13th Conf. on Fire and For. Met., Lorne, Australia, Oct. 27–31, 1997, 99012. IAWF, Fairfield, WA.
- Charlson, R.J., Schwartz, S.E., Hales, J.M., Cess, R.D., Coakley Jr., J.A., Hansen, J.E., Hoffman, D.J., 1992. Climate forcing by anthropogenic sulfate aerosols. *Science* 255, 423–430.
- Chuvieco, E., Riano, D., Aguado, I., Caceres, D., 2002. Estimation of fuel moisture content from multi-temporal analysis of LANDSAT thematic mapper reflectance data: applications in fire danger assessment. *International Journal of Remote Sensing* 23, 2145–2162.
- Dasgupta, S., Qu, J., Hao, X., Bhoi, S., 2007. Evaluating remotely sensed live fuel moisture estimations for fire behavior predictions in Georgia, USA. *Remote Sensing of Environment* 108, 138–150.
- Dickinson, R.E., Henderson-Sellers, A., Kennedy, P.J., 1993. Biosphere–Atmosphere Transfer Scheme (BATS) Version 1E as Coupled to the NCAR Community Climate Model, NCAR Tech. Note/TN-387. National Center for Atmospheric Research, Boulder, CO. 72 pp.
- Dixon, R.K., Krankina, O.N., 1993. Forest fires in Russia: carbon dioxide emissions to the atmosphere. *Canadian Journal of Forest Research* 23, 700–705.
- Englich, R.M., 1968. Objective analysis of environmental conditions associated with severe thunderstorms and tornado. *Monthly Weather Review* 96, 342–350.
- Flannigan, M.D., Bergeron, Y., Engelmark, O., Wotton, B.M., 1998. Future wildfire in circumboreal forests in relation to global warming. *Journal of Vegetation Science* 9, 469–476.
- Fosberg, M.A., 1970. Drying rates of heartwood below fiber saturation. *Forest Science* 16 (1), 57–63.
- Giorgi, F., Bates, G.T., 1989. The climatological skill of a regional model over complex terrain. *Monthly Weather Review* 117, 2325–2347.
- Giorgi, F., Bi, X., 2000. A study of internal variability of a regional climate model. *Journal of Geophysical Research* 105, 29503–29521.
- Giorgi, F., Shields, C., 1999. Tests of precipitation parameterizations available in latest version of NCAR regional climate model (RegCM) over continental United States. *Journal of Geophysical Research* 104, 6353–6375.
- Giorgi, F., Marinucci, M.R., De Canio, G., Bates, G.T., 1993a. Development of a second generation regional climate model (RegCM2), I, Boundary layer and radiative transfer processes. *Monthly Weather Review* 121, 2794–2813.
- Giorgi, F., Marinucci, M.R., De Canio, G., Bates, G.T., 1993b. Development of a second generation regional climate model (RegCM2), II, Convective processes and assimilation of lateral boundary conditions. *Monthly Weather Review* 121, 2814–2832.
- Grell, G.A., Dudhia, J., Stauffer, D.R., 1994. A Description of the Fifth Generation Penn State/NCAR Mesoscale Model (MM5), NCAR/TN-398 + STR. Natl. Cent. for Atmos. Res., Boulder, Colo. 122 pp.
- Huete, R.A., 1988. A soil-adjusted vegetation index (SAVI). *Remote Sensing of Environment* 25, 295–309.
- Jackson, R.D., 1986. Remote sensing of biotic and abiotic plant stress. *Annual Review of Phytopathology* 24, 265–287.
- Jacquemoud, S., 1993. Inversion of the PROSPECT + SAIL canopy reflectance model from AVIRIS equivalent spectra: theoretical study. *Remote Sensing of Environment* 44, 281–292.
- Karl, T.R., et al., 1988. The 1988 drought in the United States: just another drought? *EOS, Trans. American Geophysical Union* 69, 1069.
- Karl, T.R., Melillo, J.M., Peterson, T.C., 2009. Global Climate Change Impacts in the United States. Cambridge University Press, New York, p. 188.
- Keetch, J.J., Byram, G.M., 1968. A Drought Index for Forest Fire Control, USDA Forest Service, Southeast Forest Experiment Station Research Paper SE-38, Asheville. 32 pp.
- Kiehl, J.T., Hack, J.J., Bonan, G.B., Boville, B.A., Briegleb, B.P., Williamson, D.L., Rash, P.J., 1996. Description of the NCAR Community Climate Model (CCM3), NCAR/TN-420 + STR. National Center for Atmospheric Research, Boulder, CO.
- Koster, R.D., Yamada, T., Mahanama, S., Guo, Z., Dirmeyer, P.A., Van den Hurk, B.J.J.M., 2010. The Second Phase of the Global Land-Atmosphere Coupling Experiment (GLACE-2), 22nd Conference on Climate Variability and Change 24th Conference on Hydrology, Atlanta, GA, USA, January 18–21, 2010.
- Linn, R., Winterkamp, J., Edminster, C., Colman, J.J., Smith, W.S., 2007. Coupled influences of topography and wind on wildland fire behaviour. *International Journal of Wildland Fire* 16 (2), 183–195. doi:10.1071/WF06078.
- Liu, Y.-Q., 2005a. Atmospheric response and feedback to radiative forcing from biomass burning in tropical South America. *Agricultural and Forest Meteorology* 133, 40–57.
- Liu, Y.-Q., 2005b. Enhancement of the 1988 Northern U.S. drought due to wildfires. *Geophysical Research Letters* 32 (L10806). doi:10.1029/2005GL022411.
- Liu, Y.-Q., 2007. Advances in regional climate modeling. *Proceedings of Int'l Symposium on Advances in Atmospheric Science and Information Technology*, Nanjing, China, pp. 94–100.
- Liu, Y.-Q., Stanturf, J., Goodrick, S., 2009. Trends in global wildfire potential in a changing climate. *Forest Ecology and Management* 259, 685–697. doi:10.1016/j.foreco.2009.

- McDowell, N., Pockman, W.T., Allen, C.D., Breshears, D.D., Cobb, N., Kolb, T., Plaut, J., Sperry, J., West, A., Williams, D.G., Yepez, E.A., 2008. Mechanisms of plant survival and mortality during drought: why do some plants survive while others succumb to drought? *New Phytologist* 178, 719–739.
- Mearns, L.O., 2010. The North American Climate Change Assessment Program: Climate Change Results. 22nd Conference on Climate Variability and Change 24th Conference on Hydrology, Atlanta, GA, USA, January 18–21, 2010.
- Melton, M., 1989. Keetch-Byram Drought Index: a guide to fire conditions and suppression problems. *Fire Management Notes* 50 (4), 30–34.
- Moriondo, M., Good, P., Durao, R., Bindi, M., Giannakopoulos, C., Corte-Real, J., 2006. Potential impact of climate change on fire risk in the Mediterranean area. *Climate Research* 31, 85–95.
- Nelson Jr., R.M., 2000. Prediction of diurnal change in 10-h fuel stick moisture content. *Canadian Journal of Forest Research* 30, 1071–1087.
- NIFC (National Interagency Fire Center), 2010. Fire Information – Wildland Fire Statistics. http://www.nifc.gov/fire_info/fires_acres.htm.
- Page, S.E., Siegert, F., Rieley, J.O., Boehm, H.-D.V., Jaya, A., Limin, S., 2002. The amount of carbon released from peat and forest fires in Indonesia during 1977. *Nature* 420, 61–65.
- Palmer, W.C., 1965. Meteorological Drought. Research Paper No. 45. U.S. Department of Commerce Weather Bureau, Washington, D.C.
- Pyne, S., Andrews, P.L., Laven, R.D., 1996. Introduction to Wildland Fire. John Wiley & Sons, INC. 769 pp.
- Riebau, A.R., Fox, D., 2001. The new smoke management. *International Journal of Wildland Fire* 10, 415–427.
- Romme, W.H., Despain, D.G., 1989. The Yellowstone fires. *Scientific American* 261, 36–44.
- Seth, A., Giorgi, F., 1998. The effects of domain choice on summer precipitation simulation and sensitivity in a regional climate model. *Journal Climate* 11, 2698–2712.
- Shea, D.J., Trenberth, K.E., Reynolds, R.W., 1992. Global monthly sea surface temperature climatology. *Journal Climate* 5, 987–1001.
- Snyder, R.L., Spano, D., Duce, P., Baldocchi, D., Xu, L., Paw, U.K.T., 2006. A fuel dryness index for grassland fire-danger assessment. *Agricultural and Forest Meteorology* 139, 1–11.
- Tacconi, L., Moore, P.F., Kaimowitz, D., 2007. Fires in tropical forests – what is really the problem? Lessons from Indonesia. Mitigation adaptation strategies. *Global Change* 12, 55–66.
- Tucker, C.J., 1979. Red and photographic infrared linear combinations for monitoring vegetation. *Remote Sensing of Environment* 8 (2), 127–150.
- Verbesselt, A., Fleck, S., Coppin, P., 2003. Estimation of fuel moisture content towards fire risk assessment: a review. In: Viegas (Ed.), *Forest Fire Research & Wildland Fire Safety*. Millpress, Rotterdam.
- Wang, L., Qu, J., 2009. Satellite remote sensing applications for surface soil moisture monitoring: a review. *Frontiers of Earth Science in China* 3, 237–247.
- Westerling, A.L., 2004. Climate, Santa Ana winds and autumn wildfires in southern California. *Eos* 85 (31) 3 August 2004.
- Westerling, A.L., Swetnam, T., 2003. Interannual to decadal drought and wildfire in the western United States. *Eos* 84 (49), 545, 554–555.
- Xanthopoulos, G., Maher, G., Gouma, V., Gouvas, M., 2006. Is the Keetch-Byram drought index (KBDI) directly related to plant water stress? *Forest Ecology and Management* 234 (supplement 1), S27.
- Zeng, X., Dickinson, R.E., Walker, A., Shaikh, M., DeFries, R.S., Qi, J., 2000. Derivation and evaluation of global 1-km fractional vegetation cover data for land modeling. *Journal Applied Meteorology* 39, 826–839.